DAVIS: Density-Adaptive Synthetic-Vision Based Steering for Virtual Crowds

Rowan Hughes[1*] Jan Ondřej[2†] John Dingliana[1]

[1]Trinity College Dublin
[2]Disney Research, Los Angeles

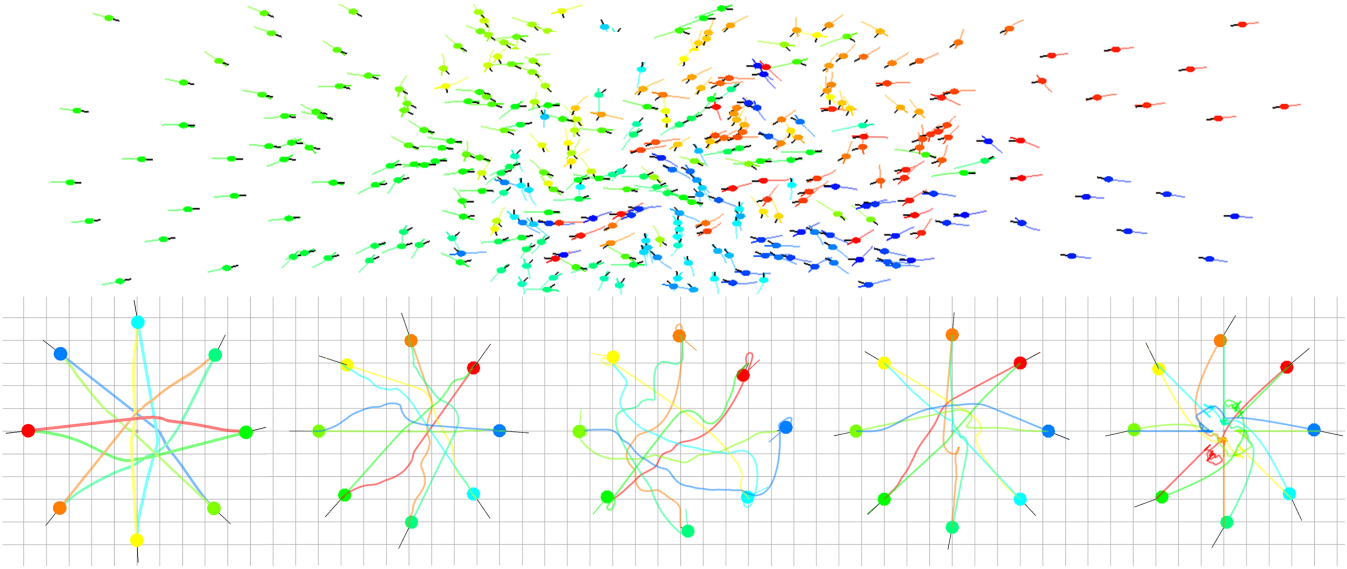

Figure 1: *(Top) A scene with 500 virtual pedestrians on a collision course, using our approach virtually no bottle-necking occurs. (Bottom) A scene containing 8 walkers all aiming to get to the diametrically opposed position. Solutions are shown for a number of models. (from right to left) Our model, Ondřej's model, Reynold's Model, RVO-Library, Helbing's Model*

Abstract

We present a novel algorithm to model density-dependent behaviours in crowd simulation. Previous work has shown that density is a key factor in governing how pedestrians adapt their behaviour. This paper specifically examines, through analysis of real pedestrian data, how density affects how agents control their rate of change of bearing angle with respect to one another. We extend upon existing synthetic vision based approaches to local collision avoidance and generate pedestrian trajectories that more faithfully represent how real people avoid each other. Our approach is capable of producing realistic human behaviours, particularly in dense, complex scenarios where the amount of time for agents to make decisions is limited.

CR Categories: I.3.7 [Computer Graphics]: Three-Dimensional Graphics and Realism—Animation I.6.5 [Simulation and Modeling]: Types of Simulation—Animation;

Keywords: Human Motion, Collision Avoidance, Virtual Agents, Simulation, Robotics

*e-mail:hughesrt@tcd.ie
†e-mail:jan.ondrej@disneyresearch.com

1 Introduction

The problem of how to simulate large scale crowds that behave realistically, particularly at high densities, remains an open problem. Crowd simulation has been extensively studied and many techniques have been advanced that aim to plausibly simulate human-like crowds. Generally these techniques are broken into two groups; global and local planners. Global avoidance planners aim to compute paths through the virtual environment to the goal position of each agent while avoiding collisions with the static obstacles in the scene. Local avoidance planners aim to allow agents to react and avoid dynamic obstacles in a scene. There exist many commonly used approaches to this aspect of collision avoidance [Helbing and Molnár 1995; van den Berg et al. 2008; Kapadia et al. 2009; Guy et al. 2010; Ondřej et al. 2010; Singh et al. 2011b; Snape et al. 2011]. Our approach aims to improve upon this aspect of path planning to produce more realistic pedestrian behaviour.

One of the key features governing how people behave in a crowd is crowd density, measured in terms of people per square meter. There have been studies across multiple disciplines investigating how agents behave with respect to density [Weidmann 1993]. These studies demonstrate the relationship between a walkers speed and density, described by the *Fundamental Diagram* [Weidmann 1993]. Recently, Best *et al.* [2014] presented their work on adapting agent velocity based on their density perception with particular respect to the agents preferred velocity.

In their work, Cutting *et al.* [1995] described their model of how pedestrians respond in order to avoid collisions. They posit that two major elements extracted from the optical flow of a pedestrian essentially governs their collision avoidance response. These ele-

ments, the perceived rate of change of bearing angle ($\dot{\alpha}$) and time-to-collision (ttc) of an obstacle are derived from the change in position and growth in size of obstacles in successively perceived images. These insights were used by Ondřej *et. al* [2010] in developing a synthetic vision based approach to local collision avoidance. In this paper, we investigate the degree to which density plays a role in decisions made due to these perceptions and adapt the synthetic-vision model to conform to our findings.

1.1 Main Results

- Through analysis of real pedestrian data we show that density plays a significant role in how agents avoid one another and affects both the tangential and angular components of velocity.
- We adapt the vision model described in [Ondřej et al. 2010] to incorporate density as a key factor in computation. We also introduce a new governing function that allows for more intuitive control over agent behaviour and that fits the observed data in a more faithful manner.
- The computational overhead of our technique is low and hardly impacts the cost of computation with respect to the original vision model.
- Our model results in smoother, more realistic trajectories and also reduces the number of collisions between agents.

The rest of the paper is organised as follows: We give a brief overview of the state of the art in Section 2. In Section 3, we present the details of the method. Section 4 outlines some of the results of our algorithm. Finally, in Section 5 we analyse the model's strengths and weaknesses.

2 Related Work

Crowd behaviour and, in particular, collision avoidance has been extensively studied across a wide variety of fields including control theory, robotics, crowd simulation, etc. In this section we give a brief overview of relevant prior work.

Local collision avoidance models for real-time multi-agent simulation fall, mainly, into a few categories including force based [Helbing et al. 2000; Pelechano et al. 2007; Karamouzas et al. 2014], rules-based [Reynolds 1999], velocity-based [Fiorini and Shillert 1998; van den Berg et al. 2008; Guy et al. 2009; Pettré et al. 2009; Berg et al. 2011], footstep driven [Singh et al. 2011b], data-driven [Lee et al. 2007; Lerner et al. 2007; Charalambous and Chrysanthou 2014] and synthetic-vision based [Ondřej et al. 2010].

Density, and its effect on crowd behaviour, is a long noted phenomenon [Wolff 1973]. There has been prior work in crowd simulation that generates *Fundamental Diagram* [Lemercier et al. 2012; He and van den Berg 2013; Bruneau et al. 2014] adherent crowd behaviour. Recently Best *et. al* [2014], presented their work, taking into consideration both psychological and physiological factors in determining their density calculation. Other approaches to pedestrian adaptation to density operate at the global-planning level [Guy et al. 2010; van Toll et al. 2012], as well as hybrid approaches such as those described by [Treuille et al. 2006; Singh et al. 2011a; Golas et al. 2013].

Our approach builds directly on the synthetic-vision based model described in [Ondřej et al. 2010]. Further advances have been made to this model including incorporating group dynamics [Wu et al. 2013] and incorporating adopting a cost based approach upon computing visual features [Dutra et al. 2014].

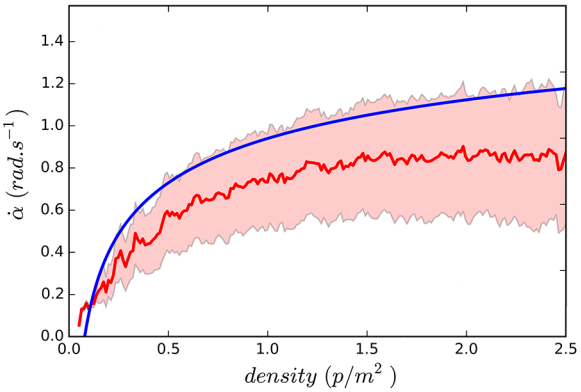

Figure 2: *Plot graphing the mean density with respect to $\dot{\alpha}$ for our dataset. ($+/-$ one standard deviation visualised by the lighter red area. The function displayed in blue represents our density function with parameters:* $(\alpha_\rho = 0.4, \beta_\rho = 0.2, \gamma_\rho = 0.85)$.

3 Method

3.1 Data Analysis

To build our model we analysed data from a set of motion-captured pedestrian trials. Each trial consisted of a number of agents set up on a rough circle and tasked to reach the diametrically opposing side. The trials consisted of between 6 and 24 pedestrians with a total of 40 trials.

Each trial dataset consisted of a set of 3D positions for the left and right shoulder markers attached to each agent, A_i, for each captured frame, f, in the trial. For each trial we construct an $N * F$ matrix, where N is the number of agents in the trial and F the number of captured frames. Each cell of the matrix c_{if}, i and f representing the current agent and frame respectively, consists of a position, speed, direction and density (p_{if},s_{if}, d_{if}, ρ_{if}), as well as parameters computed between the observed agent, A_i, and every other agent, A_j, in the trial: time-to-collision, bearing angle and rate-of-change of bearing angle (ttc_{ijf}, α_{ijf},$\dot{\alpha}_{ijf}$). Density is calculated according to the method described in [Best et al. 2014], but using observed velocity rather than "desired velocity" as this is ambiguous when dealing with real data. In order to calculate a more accurate estimate of ttc we construct a kite proxy shape using the left and right shoulder positions, with a width of $0.6m$ and a depth of $0.3m$. We then calculate ttc with respect to the closest point on the closest segment of each kite.

A pedestrian cannot simultaneously respond to all agents in dense environments, but at most a small subset. Here we make the assumption that the pedestrian responds most strongly with respect to the most imminent collision. We derive the critical time-to-collision, ttc^c_{if}, where $ttc^c_{if} = min(ttc_{ijf})$, for all $ttc_{ijf} > 0$. Using ttc^c_{if} we select α^c_{if} and $\dot{\alpha}^c_{if}$ to reduce our state vector for a given agent at a given frame to:

$$c^c_{if} = [p_{if} s_{if}, d_{if}, \rho_{if}, ttc^c_{if}, \alpha^c_{if}, \dot{\alpha}^c_{if}]. \quad (1)$$

Figure 2 shows the graph of all samples of $\dot{\alpha}^c$ plotted against ρ for $0.1 < ttc^c < 1.0$. We only look at a segment of ttc^c as ttc varies non-linearly with $\dot{\alpha}$. We discuss the implications in Section 3.3.

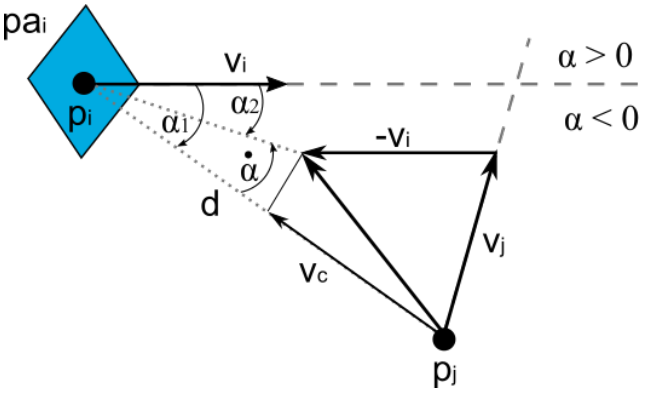

Figure 3: *$\dot{\alpha}_i$ is calculated on a per vertex basis, ttc_i on a per fragment basis. They are calculated from the relative position and velocity of the point with respect to the agent perceiving the scene.*

3.2 Model Overview

As previously mentioned, Cutting *et al.* [1995] posit that a person's avoidance behaviour is governed by two major aspects derived from their optical flow. In their work, Ondřej *et al.* [2010] leveraged these insights in developing a synthetic-vision based approach to microscopic collision avoidance. We adapt Ondřej's model to take into account density considerations when adapting agent behaviour. By using density as a key input in calculating angular velocity $\dot{\theta}_i$ we aim to create more realistic, adaptive agent behaviour.

Each agent's configuration is described by the state vector: $[pa_i, h_i, p_i, \rho_i, v_i^{curr}, v_i^{des}]^T$, where pa_i and h_i represent the scalar physical dimensions of the agent, ρ_i is the agent's density, p_i, v_i^{curr} and v_i^{des} are two dimensional vectors representing the agent's current location, velocity and desired velocity respectively. The agent's behaviour is controlled via the $(\dot{\theta}_i, v_i)$ pair, where $\dot{\theta}_i$ and v_i represent angular and tangential velocity respectively.

At each simulation step the agent's density, ρ_i, is calculated according to the method described by Best *et al.* [2014]. This value is stored and then passed to the next simulation step on the GPU. The scene is then rendered from a camera oriented to each agents perspective. Obstacles are decomposed into a set of pixels P, in exactly the manner described in [Ondřej et al. 2010]. Rather than rendering the colour channels to RGB space, we calculate for each pixel $p_i \in P$ a set of pairs $p_i \rightarrow (\dot{\alpha}, ttc_i)$ that are required to adapt agents avoidance behaviour. A parallel reduction is run on each frame to reduce its size to one pixel, representing the most "dangerous" pixel. This pixel is then used to compute $(\dot{\theta}_i, v_i)$. The details are described in the following section.

3.3 Model Description

Model inputs
The model's inputs are computed from agent's state vector and some of them are illustrated in Figure 3. We compute ttc_i and $\dot{\alpha}_i$ as follows:

$$ttc_i = d / \left\| \vec{v_c} \right\|, \tag{2}$$

$$\dot{\alpha}_i = \alpha_2 - \alpha_1. \tag{3}$$

Figure 2 shows the mean density ρ plotted against the change of bearing angle $\dot{\alpha}^c$. We can see a clear power relationship emerge between the two variables, (Note we are only observing a small slice of ttc from 0.2 to 0.4 seconds). As density decreases along the agents velocity, less adaptation is needed to achieve a collision free velocity. We model this interaction using a $densityfactor$ function δ_i defined as:

$$\delta_i = \alpha_\rho {\rho_i}^{\beta_\rho} + \gamma_\rho, \tag{4}$$

with α_ρ, β_ρ and γ_ρ representing constant parameters of the model. We found by testing that using parameters that more closely approximate values along +1 standard deviation from the mean produced the best results.

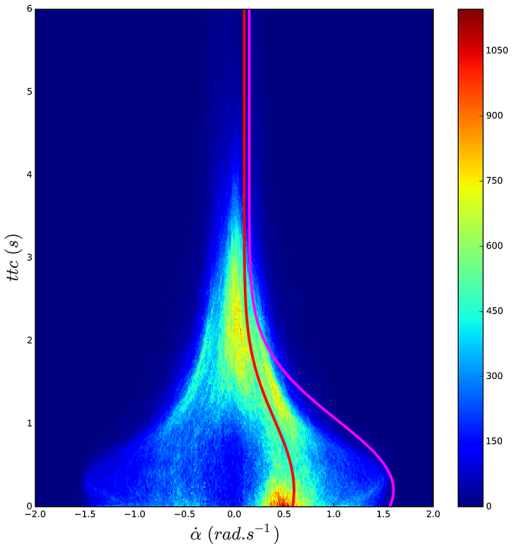

Figure 4: *2D Histogram showing $\dot{\alpha}$ plotted against ttc. This plot shows that the majority of critical, (low ttc), $\dot{\alpha}$ clusters around the $0.5(rad.s^{-1})$ mark. It also displays the propensity of agents to pass on the right hand side. Using a Gaussian-like function allows us to smoothly control the critical aspects of behaviour, but in particular it allows us to explicitly define the crossing point (peak of curve) which is derived from density information. The red and magenta curves corresponds to the parameter sets: $(\delta_i = 0.5, \alpha_{ttc} = 0.2, \sigma_{ttc} = 0.85, \beta_{ttc} = 0.05)$ and $(\delta_i = 1.5, \alpha_{ttc} = 0.2, \sigma_{ttc} = 0.85, \beta_{ttc} = 0.1)$ respectively.*

Angular Velocity Control
Once δ_i is derived we need a mechanism to use it in determining $\dot{\theta}$. Given a perceived $\dot{\alpha}$ value we describe a Gaussian-like function to determine the threshold τ under which a walker reacts:

$$\tau(ttc_i) = \delta_i \exp\left(-\frac{(ttc_i - \alpha_{ttc})^2}{2\sigma_{ttc}^2}\right) + \beta_{ttc} \tag{5}$$

where α_{ttc}, β_{ttc} and σ_{ttc} are constant parameters of the model and δ_i is our $densityfactor$ derived from (4). Figure 4 shows the 2D histogram for the pair $(\dot{\alpha}^c, ttc^c)$ for our entire dataset. As we can see the function described in (5) models the observed data smoothly, with the red and magenta curves representing low and high values for δ_i respectively.

The set of points that will be considered , $P_{col} \subset P$, is reduced as follows:

$$p_i \in P_{col} \text{ if } 0 < ttc < 6 \text{ and } \dot{\alpha}_i < \tau(ttc_i) \tag{6}$$

Having the threshold function τ and $\dot{\alpha}_i$ we can compute the angular velocity needed to avoid the collision. We define a turn to the left Φ_L and right Φ_R as follows:

$$\begin{aligned} \Phi_{Ri} &= min(\dot{\alpha}_i - \tau(ttc_i)) \\ \Phi_{Li} &= max(\dot{\alpha}_i + \tau(ttc_i)) \end{aligned} \tag{7}$$

From these two values we choose the one with a smaller amount of adaptation and use it as the angular velocity:

$$\dot{\theta}_i = \begin{cases} \Phi_{Li} & , \text{ if } |\Phi_{Li}| < |\Phi_{Ri}|, \\ \Phi_{Ri} & , \text{ otherwise.} \end{cases} \tag{8}$$

In the end, the angular velocity $\dot{\theta}_i$ is adapted by the goal position as described in [Ondřej et al. 2010].

Tangential Velocity Control
We introduce a change to the function governing speed adaptation to low ttc (9). In [Ondřej et al. 2010] the speed had been reduced to near zero for low ttc values. This would not seem to be a valid assumption, especially in dense scenarios, as if a pedestrian chooses a collision free trajectory passing closely by an obstacle a low ttc will not necessarily correspond to a large reduction in speed. Indeed investigating the data shows a marginal effect, with speed at $ttc = 0$ averaging at $1.0m/s$. With this in mind we compute clip speed accordingly:

$$v_i = (v_{comf} - 1.0) \cdot (1 - \exp^{-0.3tti^2}) + 1.0 \tag{9}$$

In addition to this we further filter the speed v using the density filter described in [Best et al. 2014] to generate a Fundamental Diagram adherent velocity.

4 Results

In this section we present the performance of our model in various scenarios. We also analyse the model, comparing and contrasting with other collision avoidance techniques.

Data Scenarios: The dataset we analysed in building our model consisted of sets of agents set up on a circle with the goal of reaching the diametrically opposite position. In Figure 5, we see real plotted trajectories for one of the trials in the dataset. This is the behaviour we are interested in reproducing.

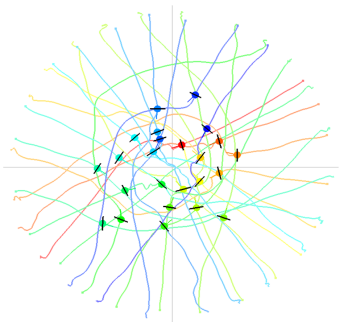

Figure 5: *Graphically illustrated example of one of the trials in our dataset.*

Figure 6 shows the emergence of natural behaviour using our approach, with agents spreading out in a plausible manner to avoid collision. We can compare this level of plausibility with that of the original Vision Model [Ondřej et al. 2010], in Figure 6(c), which tends to lead to concentric swarming behaviour. This approach does avoid bottlenecks at the centre and remains collision free but the patterns become too uniform to remain plausible. For velocity obstacle based approaches such as ORCA, Figure 6(d), this type of scenario raises major difficulties. With agents tending to converge on the centre of the circle and getting stuck there.

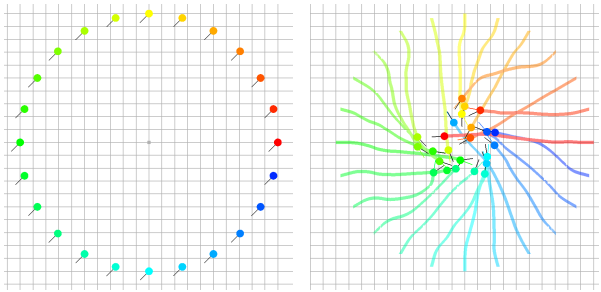

(a) Initial walker configuration (b) Our model

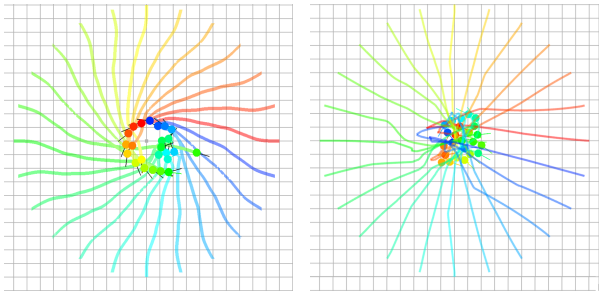

(c) Ondřej's Model (d) ORCA

Figure 6: ***Circle*** *(a) A scene of 100 walkers are initially deployed uniformly along a circle. The walker's goal is to reach the diametrically opposed position. The solution is shown for 3 models (b), (c), (d). Our model (b) is the only one able to provoke the emergence of patterns.*

Geometrically Challenging Scenarios: These simple scenarios can prove particularly difficult for velocity-obstacle based approaches due to a number of factors. In [Karamouzas et al. 2014] the authors address these challenges and show how their force based approach can solve these problems in a plausible manner. Here we show that our algorithm is similarly capable. As shown in Figure 7 we set up two basic scenarios, both of which comprise of an agent facing a block of oncoming agents (2 in the first case, 10 in the second). Figure 7(a) shows how our algorithm resolves these scenarios in a plausible manner. Figure 7(b) shows a number of other collision avoidance models attempting to resolve the same scenarios with less plausible results.

Large Scenarios: Figure 8 displays a scene in which two banks of 100 agents cross each other. Our model is scalable and can handle hundreds of agents at real-time rates. This scenario, among others, can be seen in the accompanying media.

5 Discussion

Realism The vast majority of local collision avoidance algorithms are capable of producing plausible pedestrian avoidance behaviour when considering only a small number of agents. The real challenge occurs when environments become significantly complex. The ORCA algorithm [Guy et al. 2009], while exceptionally ele-

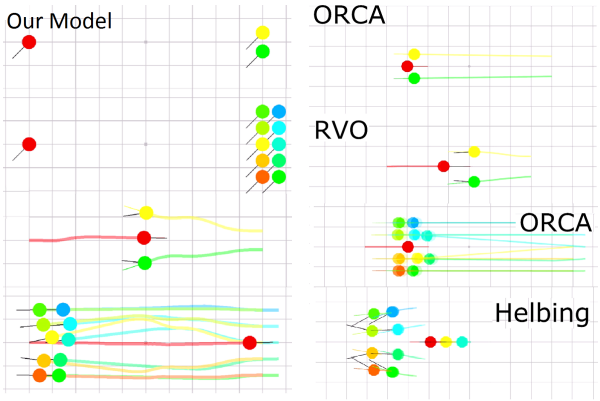

Figure 7: ***(a)*** *The top two frames represent two simple scenarios that are typically difficult for some collision avoidance algorithms to solve in a plausible manner. The bottom frames show how our algorithm solves them elegantly.* ***(b)*** *Here we run these same scenarios with a number of well known collision avoidance algorithms.*

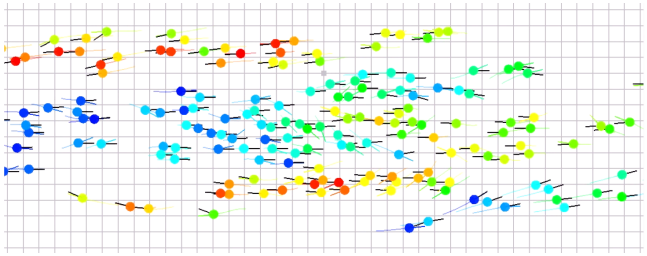

Figure 8: *A scene with two banks of walkers on opposing trajectories.*

gant, efficient and malleable [Kim et al. 2013], suffers from throwing out too much of the available solution space and guaranteeing collision free trajectories at all costs. This can lead to unusual behaviour in certain scenarios. RVO [van den Berg et al. 2008] will theoretically find a better collision free solution but suffers in terms of computational cost due to the amount of samples need to achieve this. In the field of robotics, where guaranteeing collision free path is of critical importance a vision-based approach may not be valid. Pedestrians do, however, collide from time to time particularly in very dense scenarios. Recently, we have seen force-based approaches make a re-appearance [Karamouzas et al. 2014], in their work we can see how this method overcomes some of the drawbacks seen in aforementioned algorithms. Synthetic-vision based models also avoid some of these drawbacks and sit closer to this approach; and while not guaranteeing collision free paths they do produce realistic pedestrian behaviour.

By incorporating density as a factor in determining avoidance behaviour we avoid some of the rapid and unnecessary changes in angular velocity seen when omitted. This was particularly problematic at low ttc. Agents make the adjustments necessary to avoid each other in a smooth and realistic manner.

Model Parameters In Section 3.3 we describe a novel governing function controlling our algorithm. By using a Gaussian like function we not only model the underlying data in a more faithful manner but we also gain more intuitive control over agent behaviour.

- α_{ttc}: This parameter governs the offset from $ttc = 0$ where the $\dot{\alpha}$ response reaches a maximum. We see in the data that this clusters around 0.2. This may be due to pedestrians maintaining a "safety buffer" or simply a standard error in judgement on their part.

- β_{ttc}: This parameter represents the minimum value for adaptation made by an agent on sensing a collision. This governs how generally "cautious" agents behave in simulation. (Minor changes to this variable can lead to major changes in agent behaviour.)

- σ_{ttc}: This parameter controls the degree to which adaptation is non-linear with ttc. Decreasing σ_{ttc} will reduce the point at which agents will start to significantly react to ttc.

- δ_i: This parameter is derived as outlined in Section 3.3. It governs the overall magnitude of adaptation behaviour, when density is low the adaptation is small and vice-versa.

6 Conclusion

In this paper, we analysed real pedestrian data to investigate the role that density plays in altering pedestrian behaviour. We developed a synthetic-vision based model based on these findings that incorporates crowd density as a key element in determining agent behaviour. Our approach builds upon the approach described in [Ondřej et al. 2010], and generates smoother, more realistic pedestrian trajectories.

In future work it would be interesting to investigate other types of data sets and see if our analysis holds true. We also didn't fully investigate the impact that ttc plays on tangential velocity. Partly this was due to the fact that we were looking at dense datasets, and density and tangential velocity are tightly coupled [Best et al. 2014]. In addition we are currently examining the statistical similarity between real and simulated datasets for model validation.

Acknowledgements

This research was supported by funding from the EU FP7 VERVE project (grant no. 288914) and Science Foundation Ireland project 14/TIDA/2349.

References

BERG, J., GUY, S., LIN, M., AND MANOCHA, D. 2011. Reciprocal n-body collision avoidance. In *Robotics Research*, C. Pradalier, R. Siegwart, and G. Hirzinger, Eds., vol. 70 of *Springer Tracts in Advanced Robotics*. Springer Berlin Heidelberg, 3–19.

BEST, A., NARANG, S., CURTIS, S., AND MANOCHA, D. 2014. Densesense: Interactive crowd simulation using density-dependent filters. In *Symposium on Computer Animation*, 97–102.

BRUNEAU, J., DUTRA, T. B., AND PETTRÉ, J. 2014. Following behaviors: A model for computing following distances based on prediction. In *Proceedings of the Seventh International Conference on Motion in Games*, ACM, New York, NY, USA, MIG '14, 17–24.

CHARALAMBOUS, P., AND CHRYSANTHOU, Y. 2014. The pag crowd: A graph based approach for efficient data-driven crowd simulation. *Comput. Graph. Forum 33*, 8 (Dec.), 95–108.

CUTTING, J. E., VISHTON, P. M., AND BRAREN, P. A. 1995. How we avoid collisions with stationary and with moving obstacles. *Psychological Review 102*, 627–651.

DUTRA, T. B., PRIEM, G., CAVALCANTE-NETO, J. B., VIDAL, C. A., AND PETTRÉ, J. 2014. Synthetic Vision-based Crowd Simulation: Reactive vs. Reactive Planning Approaches. In *Proceedings of the 27th Conference on Computer Animation and Social Agents (CASA 2014)*.

FIORINI, P., AND SHILLERT, Z. 1998. Motion planning in dynamic environments using velocity obstacles. *International Journal of Robotics Research 17*, 760–772.

GOLAS, A., NARAIN, R., AND LIN, M. 2013. Hybrid long-range collision avoidance for crowd simulation. In *Proceedings of the ACM SIGGRAPH Symposium on Interactive 3D Graphics and Games*, ACM, New York, NY, USA, I3D '13, 29–36.

GUY, S. J., CHHUGANI, J., KIM, C., SATISH, N., LIN, M., MANOCHA, D., AND DUBEY, P. 2009. Clearpath: highly parallel collision avoidance for multi-agent simulation. In *Proceedings of the 2009 ACM SIGGRAPH/Eurographics Symposium on Computer Animation*, ACM, New York, NY, USA, SCA '09, 177–187.

GUY, S. J., CHHUGANI, J., CURTIS, S., DUBEY, P., LIN, M., AND MANOCHA, D. 2010. Pledestrians: a least-effort approach to crowd simulation. In *Proceedings of the 2010 ACM SIGGRAPH/Eurographics Symposium on Computer Animation*, Eurographics Association, Aire-la-Ville, Switzerland, Switzerland, SCA '10, 119–128.

HE, L., AND VAN DEN BERG, J. 2013. Meso-scale planning for multi-agent navigation. In *2013 IEEE International Conference on Robotics and Automation, Karlsruhe, Germany, May 6-10, 2013*, 2839–2844.

HELBING, D., AND MOLNÁR, P. 1995. Social force model for pedestrian dynamics. *Phys. Rev. E 51* (May), 4282–4286.

HELBING, D., FARKAS, I., AND VICSEK, T. 2000. Simulating dynamical features of escape panic. *Nature*, 2000.

KAPADIA, M., SINGH, S., HEWLETT, W., AND FALOUTSOS, P. 2009. Egocentric affordance fields in pedestrian steering. In *Proceedings of the 2009 Symposium on Interactive 3D Graphics and Games*, ACM, New York, NY, USA, I3D '09, 215–223.

KARAMOUZAS, I., SKINNER, B., AND GUY, S. J. 2014. Universal power law governing pedestrian interactions. *Phys. Rev. Lett. 113* (Dec), 238701.

KIM, S., GUY, S. J., AND MANOCHA, D. 2013. Velocity-based modeling of physical interactions in multi-agent simulations. In *Proceedings of the 12th ACM SIGGRAPH/Eurographics Symposium on Computer Animation*, ACM, New York, NY, USA, SCA '13, 125–133.

LEE, K. H., CHOI, M. G., HONG, Q., AND LEE, J. 2007. Group behavior from video: a data-driven approach to crowd simulation. In *Proceedings of the 2007 ACM SIGGRAPH/Eurographics symposium on Computer animation*, Eurographics Association, Aire-la-Ville, Switzerland, Switzerland, SCA '07, 109–118.

LEMERCIER, S., JELIC, A., KULPA, R., HUA, J., FEHRENBACH, J., DEGOND, P., APPERT-ROLLAND, C., DONIKIAN, S., AND PETTRé, J. 2012. Realistic following behaviors for crowd simulation. *Comp. Graph. Forum 31*, 2pt2 (May), 489–498.

LERNER, A., CHRYSANTHOU, Y., AND LISCHINSKI, D. 2007. Crowds by example. *Comput. Graph. Forum 26*, 3, 655–664.

ONDŘEJ, J., PETTRÉ, J., OLIVIER, A.-H., AND DONIKIAN, S. 2010. A synthetic-vision based steering approach for crowd simulation. In *ACM SIGGRAPH 2010 papers*, ACM, New York, NY, USA, SIGGRAPH '10, 123:1–123:9.

PELECHANO, N., ALLBECK, J. M., AND BADLER, N. I. 2007. Controlling individual agents in high-density crowd simulation. In *Proceedings of the 2007 ACM SIGGRAPH/Eurographics symposium on Computer animation*, Eurographics Association, Aire-la-Ville, Switzerland, Switzerland, SCA '07, 99–108.

PETTRÉ, J., ONDŘEJ, J., OLIVIER, A.-H., CRETUAL, A., AND DONIKIAN, S. 2009. Experiment-based modeling, simulation and validation of interactions between virtual walkers. In *Proceedings of the 2009 ACM SIGGRAPH/Eurographics Symposium on Computer Animation*, ACM, New York, NY, USA, SCA '09, 189–198.

REYNOLDS, C., 1999. Steering behaviors for autonomous characters.

SINGH, S., KAPADIA, M., HEWLETT, B., REINMAN, G., AND FALOUTSOS, P. 2011. A modular framework for adaptive agent-based steering. In *Symposium on Interactive 3D Graphics and Games*, ACM, New York, NY, USA, I3D '11, 141–150.

SINGH, S., KAPADIA, M., REINMAN, G., AND FALOUTSOS, P. 2011. Footstep navigation for dynamic crowds. In *Symposium on Interactive 3D Graphics and Games*, ACM, New York, NY, USA, I3D '11, 203–203.

SNAPE, J., VAN DEN BERG, J., GUY, S., AND MANOCHA, D. 2011. The hybrid reciprocal velocity obstacle. *Robotics, IEEE Transactions on 27*, 4, 696–706.

TREUILLE, A., COOPER, S., AND POPOVIĆ, Z. 2006. Continuum crowds. In *ACM SIGGRAPH 2006 Papers*, ACM, New York, NY, USA, SIGGRAPH '06, 1160–1168.

VAN DEN BERG, J., LIN, M. C., AND MANOCHA, D. 2008. Reciprocal velocity obstacles for real-time multi-agent navigation. In *IEEE INTERNATIONAL CONFERENCE ON ROBOTICS AND AUTOMATION*, IEEE, 1928–1935.

VAN TOLL, W. G., COOK, IV, A. F., AND GERAERTS, R. 2012. Real-time density-based crowd simulation. *Comput. Animat. Virtual Worlds 23*, 1 (Feb.), 59–69.

WEIDMANN, U. 1993. *Transporttechnik der Fussgänger: transporttechnische Eigenschaften des Fussgängerverkehrs ; Literaturauswertung*. Schriftenreihe des IVT. IVT.

WOLFF, M. 1973. Notes on the behavior of pedestrians. *People In Places: The Sociology Of The Familiar.*, 35–48.

WU, Q., JI, Q., DU, J., AND LI, X. 2013. Simulating the local behavior of small pedestrian groups using synthetic-vision based steering approach. In *Proceedings of the 12th ACM SIGGRAPH International Conference on Virtual-Reality Continuum and Its Applications in Industry*, ACM, New York, NY, USA, VRCAI '13, 41–50.